

RESEARCH ARTICLE SUMMARY

NEURODEVELOPMENT

Branch-restricted localization of phosphatase Prl-1 specifies axonal synaptogenesis domains

Olivier Urwyler*, Azadeh Izadifar, Sofie Vandenbergaeerde, Sonja Sachse, Anke Misbaer, Dietmar Schmucker*

INTRODUCTION: Axons grow collateral branches to project to distinct target areas in the central nervous system (CNS) and to form synapses with various postsynaptic partner cells. Synapse numbers, locations, and types can differ in different axon collaterals of the same neuron and need to be specified independently in each collateral. Which mechanisms control synapse formation with subcellular and spatial specificity in the CNS? Signaling dependent on cell surface receptors is essential in the processes of axon guidance, branching, and synaptogenesis. However, how intracellular axon-intrinsic factors control compartment-specific synaptogenesis in the CNS remains unclear.

RATIONALE: Using a genetic single-cell approach that allows the labeling and manipula-

tion of single, specific mechanosensory axons in the *Drosophila* CNS, we searched for molecular players controlling synapse formation specifically in one subcellular compartment and target area. Protein kinases and phosphatases control reversible phosphorylation cascades that are central to most intracellular signaling pathways. We reasoned that these kinases and phosphatases are likely also key to controlling the spatial specificity of synapse formation and screened the fly kinome and phosphatome by an *in vivo* cell-autonomous knockdown approach.

RESULTS: We found that the loss of phosphatase of regenerating liver (Prl-1) specifically reduces synapses organized in a terminal arbor in one target area of mechanosensory neurons. Collaterals that target other CNS

regions do not display axonal or synaptic defects. Prl family members are small, membrane-localized phosphatases conserved from invertebrates to mammals. They are associated with metastatic progression of tumors. Prl genes are also expressed in the CNSs of flies and mice; however, their neuronal functions are not known. In this study, we show that the loss of *Drosophila* Prl-1 leads to defects in axonal target areas in several CNS circuits. The CNS of *prl-1* null mutant flies is reduced in size, and the animals have locomotor defects. A developmental analysis in mechanosensory neurons revealed that Prl-1 is required for

ON OUR WEBSITE

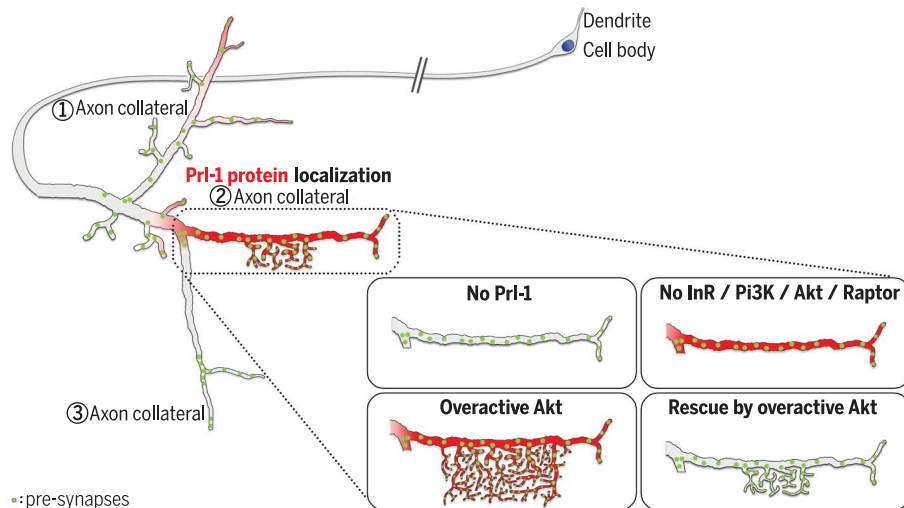
Read the full article at <http://dx.doi.org/10.1126/science.aau9952>

the stabilization of nascent axonal arbors and synaptic structures. Prl-1 overexpression induces ectopic axonal protrusions and synapses. Prl proteins are dual-specificity phosphatases, and human Prl-3 was suggested to

dephosphorylate not only protein substrates but also the phosphoinositide phosphatidylinositol 4,5-bisphosphate [PI(4,5)P₂]. We provide genetic evidence consistent with the model that Prl-1 leads to the reduction of PI(4,5)P₂ in the process of local synaptogenesis.

Moreover, our data show that the synaptogenic function of Prl-1 involves axon branch-specific modulation of the insulin receptor (InR) signaling pathway. Reduction of InR, phosphatidylinositol 3-kinase, Akt, or Raptor, presynaptically, phenocopies the branch-specific loss of synaptic arborizations. Conversely, the knockdown of PTEN or the expression of constitutively active Akt substantially increases the number of presynapses, an effect that can be suppressed by the loss of Prl-1. Therefore, inactivation of this signaling cascade produces the same spatially restricted synaptic defects as the loss of Prl-1. Lastly, we show that Prl-1 protein gets selectively localized to the axon compartment in which its function is required. Compartment-specific localization and function of Prl-1 depend on long untranslated sequences in the *prl-1* mRNA.

CONCLUSION: Prl phosphatase regulates CNS circuit formation. Prl-1 modulates InR-Akt signaling, likely by targeting membrane phosphoinositides, to control synapse formation specifically in one axon collateral of mechanosensory neurons. We suggest that untranslated *prl-1* mRNA elements could mediate the local translation of Prl-1 in axonal subcompartments. Thus, Prl-1 could provide a specificity factor to restrict Akt signaling and synapse formation in a subcellular compartment of neurons. ■



Axon branch-specific localization of Prl-1 directs CNS synaptogenesis. Mechanosensory axons innervate distinct CNS target areas by forming three primary collaterals (1 to 3). Each collateral assembles specific types and numbers of synapses. Prl-1 phosphatase and the InR-Akt signaling pathway are specifically required for the formation of terminal arbor synapses in the contralateral collateral (2), and exuberant synaptogenesis is induced by activated Akt in this collateral. The loss of Prl-1 can be rescued by active Akt. Prl-1 protein is enriched in axon collateral 2, thereby providing spatial specificity. PI3K, phosphatidylinositol 3-kinase.

The list of author affiliations is available in the full article online.
*Corresponding author. Email: dietmar.schmucker@kuleuven.vib.be (D.S.); olivier.urwyler@uzh.ch (O.U.)
Cite this article as O. Urwyler et al., *Science* 364, eaau9952 (2019). DOI: 10.1126/science.aau9952

RESEARCH ARTICLE

NEURODEVELOPMENT

Branch-restricted localization of phosphatase Prl-1 specifies axonal synaptogenesis domains

Olivier Urwyler^{1,2*}, Azadeh Izadifar^{1,3}, Sofie Vandenberghe¹, Sonja Sachse¹, Anke Misbaer^{1,3}, Dietmar Schmucker^{1,3*}

Central nervous system (CNS) circuit development requires subcellular control of synapse formation and patterning of synapse abundance. We identified the *Drosophila* membrane-anchored phosphatase of regenerating liver (Prl-1) as an axon-intrinsic factor that promotes synapse formation in a spatially restricted fashion. The loss of Prl-1 in mechanosensory neurons reduced the number of CNS presynapses localized on a single axon collateral and organized as a terminal arbor. Flies lacking all Prl-1 protein had locomotor defects. The overexpression of Prl-1 induced ectopic synapses. In mechanosensory neurons, Prl-1 modulates the insulin receptor (InR) signaling pathway within a single contralateral axon compartment, thereby affecting the number of synapses. The axon branch-specific localization and function of Prl-1 depend on untranslated regions of the *prl-1* messenger RNA (mRNA). Therefore, compartmentalized restriction of Prl-1 serves as a specificity factor for the subcellular control of axonal synaptogenesis.

Central nervous system (CNS) function relies on controlled axon branching and synapse formation during development. The establishment of neuronal circuits requires matching of pre- and postsynaptic neurons, determination of synapse locations and numbers, and specification of diverse synapse types (1, 2). The formation of multiple axon branches allows single CNS neurons to innervate several different target areas and target cells, thereby increasing output complexity (3, 4). However, for each axon branch, the quantity of synapses formed determines the number of potential postsynaptic partners and the strength of connectivity to each of them. Branch-specific control of synapse numbers is therefore essential for correct and complex circuit formation. Although synapses can be formed en passant on primary axon branches, the formation of terminal arborizations allows for more synapses in a particular location (5). In developing axons of both vertebrates and invertebrates, the localization of presynaptic proteins, as well as axonal RNAs and mitochondria, is associated with the emergence of filopodial protrusions and their stabilization into nascent branches (5–9), including the stabilization of arbors by synaptic adhesion complexes (10). Thus, terminal arborization and synaptogenesis together lead to the formation of local synapse-dense axon terminals.

Cell surface receptors mediate cell-cell communication and sensing of environmental cues during axon guidance, branching, and synapse formation (3, 11–13). For example, “neuritic adhesion complexes,” containing neuroligin and neu-rexin and presynaptic proteins Syd1 and liprin- α , locally stabilize filopodia, establishing distinct axon arborizations (10). Less is known about cell-intrinsic factors that locally control terminal arborization and synaptogenesis in vivo (4). In this study, we used a genetic single-cell approach in *Drosophila* to identify a factor that functions in the formation of dense, synapse-rich terminal arbors specifically in one collateral of a CNS axon.

We found differences in arborizations and synapse numbers formed by individual axon collaterals of single mechanosensory neurons in the *Drosophila* CNS. We focused on two types of mechanosensory neurons that innervate large sensory bristles on the dorsal thorax of the fly [scutellar (SC) and dorsocentral (DC) bristles] (Fig. 1A). These mechanosensory neurons form three main central axonal projections to innervate anterior, posterior, and contralateral CNS target areas (Fig. 1B). In DC neurons, en passant synapses that form directly on the axon shaft are predominant in the main anterior projection, which in addition forms a few variable higher-order processes that sprout from the main branch and contain terminal synapses (Fig. 1D). The posterior projection has few terminal or side arbors and forms only a few en passant synapses at an intermediate and distal position [Fig. 1D; see also (14)]. The contralateral projection of DC neurons is rich in both en passant and terminal synapses that form on an extensive network of

arborizations across the region of the CNS midline and contralaterally (Fig. 1, D and H). The extensive synaptic arborizations are present only in DC neurons [anterior DC (aDC) and posterior DC (pDC) neurons] and not in the closely related SC mechanosensory neurons, although their target areas overlap almost perfectly (Fig. 1, B and C). Therefore, mechanosensory neurons provide an in vivo model for studying the mechanisms underlying the quantitative and subcellular restriction of presynapse formation.

Prl-1 function regulates the formation of synapse-dense terminal arbors

Reversible phosphorylation cascades often regulate cellular signal transduction. We therefore targeted the kinase and phosphatase of *Drosophila* to scan for signaling factors that control synaptogenic regulatory mechanisms. RNA interference (RNAi) constructs (15) were driven in a restricted set of peripheral mechanosensory neurons as described [see experimental procedures in the supplementary materials and (14)]. We assessed phenotypes caused by cell-autonomous depletion of the target gene products in mechanosensory neurons. Among a set of synaptogenic candidates, we found that the knockdown of *phosphatase of regenerating liver (prl-1)* eliminated the terminal arbor and reduced the numbers of synapses in the contralateral projecting axon collateral (Fig. 1, E and I), whereas en passant synapses along the axon shaft and synapses in the other two main axon collaterals were unaffected (Fig. 1, E and I). Terminal arbor and bouton formation at *Drosophila* neuromuscular junctions (NMJs) appeared to be unaffected (see fig. S8). The *Drosophila* genome includes a single *prl* gene; three *Prl* genes (*Prl-1* to *-3*) are found in vertebrates (16, 17). We generated *prl-1* loss-of-function alleles by CRISPR-Cas9-mediated gene editing. In six mutant alleles (fig. S1, A and B), the stop codons are close to the start ATG codon, and no Prl-1 protein could be detected in the mutants by antibody staining (fig. S1C). We consider these six alleles to be protein null mutants. *prl-1* null flies are viable and fertile, although hatching is delayed (fig. S1D). Consistent with the RNAi knockdown, synaptic arborizations were lost from the contralateral mechanosensory neuron axon collateral in *prl-1* mutant animals (Fig. 1, F, J, M, and N). Cell body morphology, axon caliber (fig. S3), and axon growth and guidance to the CNS were unaffected. Projections of the related SC mechanosensory neurons were normal (fig. S4). The DC neuron mutant phenotype was fully rescued by the introduction of a *prl-1* BAC (bacterial artificial chromosome) transgene (Fig. 1, G and K). Anterior and posterior branches of the mechanosensory neuron arbor did not show any morphological defects in the mutants, indicating that *prl-1* is specifically required for the formation of dense synaptic terminal arborizations in one out of three main mechanosensory neuron axon collaterals. We estimated numbers of presynaptic active zones by quantifying puncta of the active zone marker Bruchpilot (Brp) (18, 19) and found an approximate decrease by 65% of synapses in the

¹VIB Center for Brain and Disease Research, Leuven, Belgium. ²Institute of Molecular Life Sciences, University of Zurich, 8057 Zurich, Switzerland. ³Department of Neurosciences, KU Leuven, Leuven, Belgium.

*Corresponding author. Email: dietmar.schmucker@kuleuven.vib.be (D.S.); olivier.urwyler@uzh.ch (O.U.)

Fig. 1. Loss of *prl-1* disrupts the formation of synapse-dense terminal arbors specifically in one axon collateral. (A) The locations of pDC and anterior SC (aSC) large bristles on the fly thorax. (B) Central axon projections of mechanosensory neurons innervating the pDC and aSC bristles in the adult animal. Boxes indicate a central region of the contralateral collateral [see (C)]. In this and all subsequent figures, the top represents anterior and the bottom represents posterior. (C) The DC axon collateral that projects to the contralateral side of the CNS has formed dense terminal arborizations, whereas the same axon collateral of the SC neuron has not (arrows). (D) Axon (CD8.GFP) (red) and pre-synapse (Cherry.Syt1) (green) markers expressed in a single DC neuron and visualized by immunostaining. Neural cadherin (NCad) (blue) is used for neuropil staining. Three primary axon collaterals innervate distinct areas of the CNS (1, anterior; 2, contralateral; 3, posterior) with different numbers of synapses. Note the extensive Syt1 labeling in the terminal arbors of the contralateral axon branch (arrow). (E) DC neuron in which *prl-1* was knocked down by RNAi. Terminal arbors are strongly reduced or virtually absent in the contralateral branch (arrow), whereas the two collaterals that innervate the other main target areas are unaffected. (F) Terminal arbors are completely lost from the contralateral branch in a whole-animal *prl-1* mutant (arrow), whereas the other target areas are unaffected. (G) The arbor loss phenotype is rescued by the introduction of a transgenic BAC containing *prl-1*. (H to K) Magnification of the DC neuron contralateral axon collateral in the indicated genotypes, illustrating the loss of terminal synaptic arborizations upon *prl-1* knockdown or loss of function [(I) and (J)]. CD8.GFP and Cherry.Syt1 signals are reconstructed with Imaris software for panels (H'') to (K). (L and M) Schematics illustrating the three target areas innervated by the main axon collaterals of mechanosensory neurons, the different amounts and types of synapses formed, and the loss of synaptic arborizations in *prl-1* null animals (arrows). (N) The territory occupied by terminal arbors on the contralateral branch is strongly reduced in different whole-animal *prl-1* mutant combinations (ns/Df, nonsense mutation over deficiency; ms, missense mutation) (see

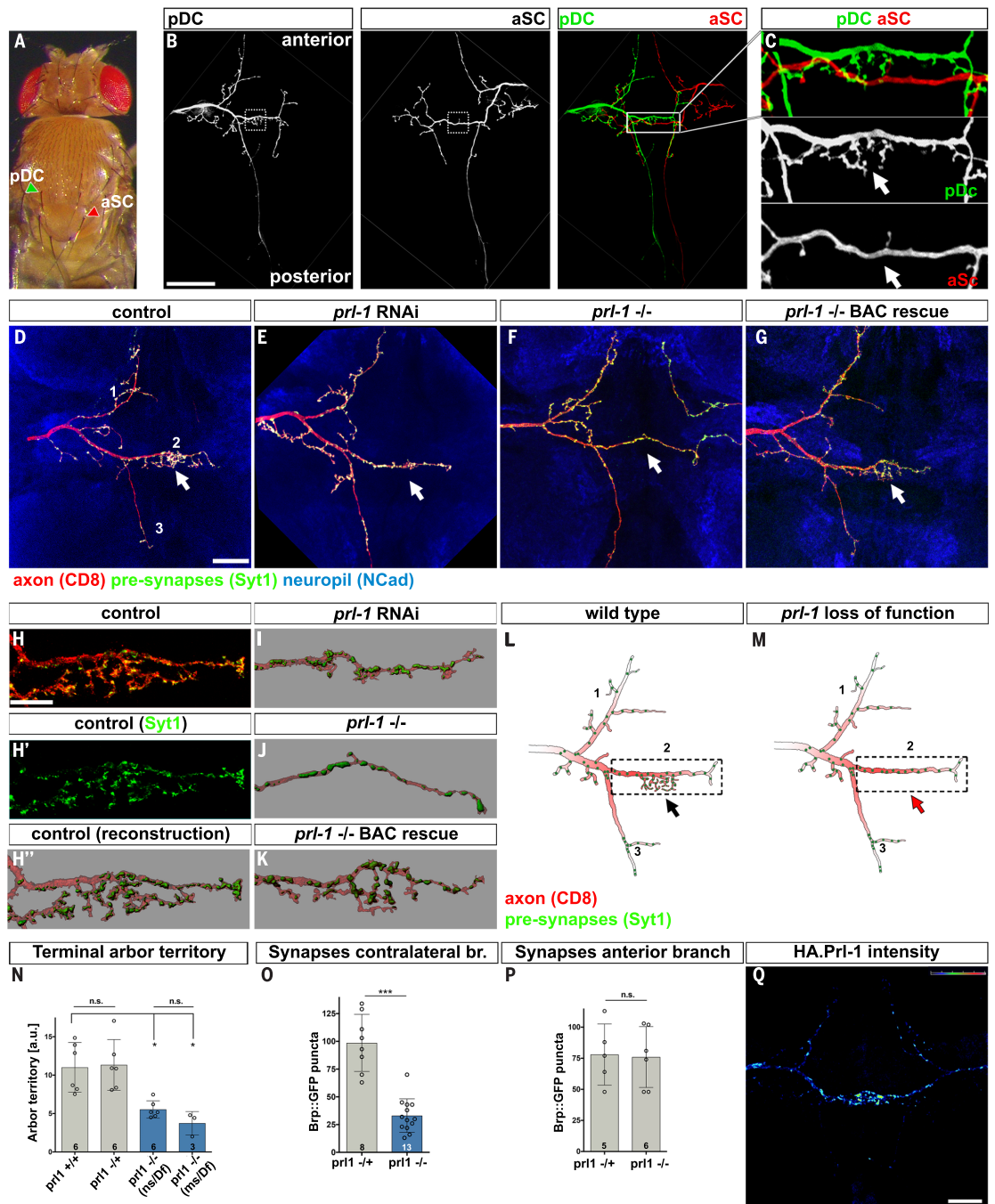


fig. S1 for the mutations and fig. S2 for the quantification method). a.u., arbitrary units; n.s., nonsignificant. * $P < 0.05$, Kruskal-Wallis test with multiple comparisons. (O) Synapse numbers, as assessed by counting puncta of the Brp^{short}:GFP marker (42) expressed in single DC neurons, are significantly decreased in the contralateral branch (br.) upon the loss of *prl-1* (Mann-Whitney test, $P < 0.0001$) (see fig. S5 for example images of samples used for quantification). (P) Synapse numbers are not altered in the anterior target area 1 upon the loss of *prl-1* (Mann-Whitney test, n.s.). (Q) HA-tagged Prl-1 protein is enriched in contralateral axon collaterals of DC neurons (false-color intensity display; blue, low levels; yellow-red, high levels). Scale bars: (B), 50 μ m; (D) and (Q), 20 μ m; and (H), 10 μ m. In the graphs in this and all subsequent figures, individual measured values and the mean are displayed, and error bars indicate SD. Genotypes for all panels can be found in table S1.

contralateral branch, whereas synapse numbers in the anterior branch were not altered (Fig. 1, O and P, and fig. S5). Consistent with a role for Prl-1 in only the axon compartment of the contralateral branch, hemagglutinin (HA)-tagged transgenic Prl-1 specifically expressed in DC neurons is enriched in this axon collateral compartment (Fig. 1Q). Correlative light and electron microscopy confirmed the labeling of presynapses by the markers [see also (14)]. No defects were apparent in the structure of the remaining synapses in the mutant (fig. S6).

Homozygous *prl-1* mutant adults are normal in size and morphology (fig. S1, E and F) but occasionally show a “held-up” wing phenotype (see movie S1). However, the mutant flies display locomotor defects and cannot fly (fig. S7, A to C, and movie S1). Our analysis of the morphology of NMJ synapses shows no defect, suggesting that *prl-1* is not required for NMJ formation (fig. S8). By contrast, analysis of the brain and CNS revealed altered synaptic connectivity in several circuits in homozygous *prl-1* mutant flies (figs. S7, S9, and S10). First, two distinct brain neuropils related to olfaction and olfaction-associated learning, the antennal lobes and mushroom bodies, respectively, were disorganized, with evident axonal or synaptic defects (figs. S7, E and G, and S9). For example, we found changes in the size and organization of synaptic termination zones of odorant receptor neurons in their target area, the glomeruli of the antennal lobe (fig. S7, E, G, and I). Second, although cell numbers of the sensory neurons (fig. S7, D, F, and H), as well as neurons of the ventral nerve cord (VNC) (fig. S10, D and E), are unaltered, the size of the CNS neuropil (a region of densely packed axons, dendrites, and synapses) is reduced in *prl-1* homozygous adult flies (fig. S10, A to C). We noted a size reduction particularly of the metathoracic neuropil in the VNC, which is smaller in homo- or hemizygous *prl-1* null mutants than in wild-type flies or *prl-1* null mutants rescued with the BAC transgene.

To test whether an increase of Prl-1 function (i.e., gain of function) could promote ectopic synapse formation, we overexpressed Prl-1 in mechanosensory neurons in otherwise wild-type animals (Fig. 2). We found an aberrant increase in synaptotagmin-1 (Syt1) puncta in ectopic proximal regions of the main axon, a region that rarely contains presynapses in controls (Fig. 2, A, B, and E to H). In addition, axon terminals of Prl-1-overexpressing neurons appeared less mature than controls and resembled axonal protrusions occurring during synapse formation at developing stages. Small protrusions were observed on the main branch (Fig. 2F), and even longer ones in terminal regions (Fig. 2D). These filopodial protrusions cannot be detected in control samples (Fig. 2, C and E). Ectopic protrusions were associated with Syt1 marker puncta, which were located either at the base or within the protrusion (Fig. 2F’). These findings suggest that Prl-1 is capable of inducing ectopic synapses. However, an increase of synapses is not seen throughout the entire axonal arbor, indicating

constraints in the synaptogenic function of Prl-1. The formation of ectopic synapses through the gain of Prl-1 is not linked to an increase in ectopic branches or terminal arbors. This suggests that Prl-1 is involved in synapse formation or stabilization rather than terminal arbor formation (branching).

Prl-1 function involves modulation of InR to Akt signaling

In our attempts to identify regulators or targets of Prl-1 phosphatase, we conducted a secondary candidate screen and discovered that cell-autonomous inhibition of multiple insulin receptor (InR) signaling components resulted in *prl-1*-like phenotypes (Fig. 3). The RNAi-based knockdown of InR in mechanosensory neurons or the expression of a dominant-negative form of the InR led to pronounced reduction of terminal synapses on the contralateral axon compartment of DC neurons (Fig. 3B, top panels). The same was observed for the knockdown of *chico* (encoding a *Drosophila* InR substrate), phosphatidylinositol 3-kinase (PI3K) (by targeting either the p110 or the p60 subunit), Akt, and the mTORC1 (mechanistic target of rapamycin complex 1) subunit Raptor (Fig. 3, B, D, and E, and figs. S11 and S12). Consistent with the finding that the knockdown of PTEN (phosphatase and tensin homolog), a negative regulator of the pathway, increases terminal synaptic arborizations on the contralateral branch, the expression of a membrane-targeted, constitutively active form of Akt (20) led to the expansion of synaptic terminals (Fig. 3, A, B, and D). We also tested the knockdown of Pdk but found no synaptic defect, suggesting that Pdk does not participate in this presynaptic signaling cascade (fig. S13). All the above-mentioned manipulations affected the contralateral projecting axon collateral but not the main axon shaft or other collaterals of DC neurons (Fig. 3A and fig. S12).

As the loss of *prl-1* leads to the same loss of terminal synapses as the reduction in InR-Akt signaling, we performed three experiments to test for genetic interactions and epistasis. First, we knocked down PTEN in *prl-1* heterozygous mutant animals and observed a suppression of exuberant arborizations upon PTEN knockdown alone (Fig. 3, C and D, and figs. S11 and S12). Second, we expressed constitutively active Akt in mechanosensory neurons of *prl-1* null animals. This led to a rescue of terminal synapses in the contralateral branch (Fig. 3, C and D, and figs. S11 and S12). Third, and conversely, we tested whether defects from the loss of Akt remained dominant over upstream activation sequence (UAS)-Prl-1 expression. UAS-Prl-1 expression showed no rescuing effect in mechanosensory neurons depleted of Akt (Fig. 3D), consistent with Akt being downstream of Prl-1.

All our genetic studies are also consistent with previous findings of high-throughput screens targeting the kinase-phosphatase signaling networks in vitro. Combined genome-wide RNAi and proteomics screens in *Drosophila* cells suggested that the activity of Prl phosphatases might be linked to InR signaling (21), and several verte-

brate cell culture studies provided evidence for a role of Prl phosphatases in PI3K-PTEN and Akt signaling (22, 23).

Thus, we suggest that compartmentalized *prl-1* activity regulates a spatially specific mode of synaptogenesis in terminal arbors via modulation of the InR pathway, likely upstream of Akt.

Targeting phosphoinositide levels affects terminal arbors

Prl phosphatases have various potential protein targets, such as the ERM (ezrin-radixin-moesin) protein ezrin or a Rho-guanosine triphosphatase-activating protein (16), although RNAi-based knockdown of several proposed protein targets provided no evidence of their involvement in Prl-1-related functions in synapse formation (fig. S14). Vertebrate Prl phosphatases can dephosphorylate phospholipids in vitro: Human Prl-3 has a PI(4,5)P2 (phosphatidylinositol 4,5-bisphosphate) 5-phosphatase activity, dephosphorylating PI(4,5)P2 to PI(4)P (phosphatidylinositol 4-phosphate) (24). Moreover, phospholipids directly regulate Akt signaling (Fig. 3E). Akt is recruited to the plasma membrane and activated by phosphatidylinositol 3,4,5-trisphosphate and phosphatidylinositol 3,4-bisphosphate (25, 26). PTEN is itself activated by PI(4,5)P2 (27).

We therefore tested whether the dephosphorylation of PI(4,5)P2 could be relevant in vivo during synapse formation of DC neurons. We reasoned that a loss of Prl-1 activity could cause an increase of local PI(4,5)P2 levels and that an increase of PI(4,5)P2 levels in DC neurons could also be achieved by promoting the phosphorylation of PI(4)P by a PI(4)P-specific kinase. The *Drosophila* PI(4)P 5-kinase Skittles (Sktl) catalyzes PI(4)P phosphorylation to PI(4,5)P2 (28–30). Therefore, Sktl overexpression in DC neurons might be equivalent to the loss of Prl-1. We found that Sktl overexpression in DC neurons leads to a reduction of terminal arborizations, phenocopying *prl-1* loss of function (Fig. 4, A to C). Moreover, coexpression of Prl-1 and Sktl suppresses the Sktl gain-of-function phenotype (Fig. 4, A and C). This result supports the idea that the Prl-1 phosphatase and Sktl kinase can carry out opposing functions and is consistent with the hypothesis that PI(4,5)P2 levels could be decreased by Prl-1 function in vivo.

In amino acid sequence, *Drosophila* Prl-1 shares features with human Prl-3 that are thought to affect activity toward phosphoinositides (fig. S15). The point mutation Gly¹²⁹→Glu (G129E) in human PTEN and the mutation Ala¹¹¹→Ser (A111S) in human Prl-3 abolish phosphatase activity toward phosphoinositides but not toward phosphoproteins of these related phosphatases (24, 31). We therefore generated transgenes with the corresponding mutations in *Drosophila* Prl-1 (G114E and A116S, respectively) and tested their ability to rescue the *prl-1* null phenotype in DC neurons. Although mechanosensory neuron-specific expression of a wild-type transgene rescued the loss of terminal arborizations (Fig. 4, D and E), expression of the G114E mutant transgene did not (Fig. 4, D and E, and fig. S16). In this experiment,

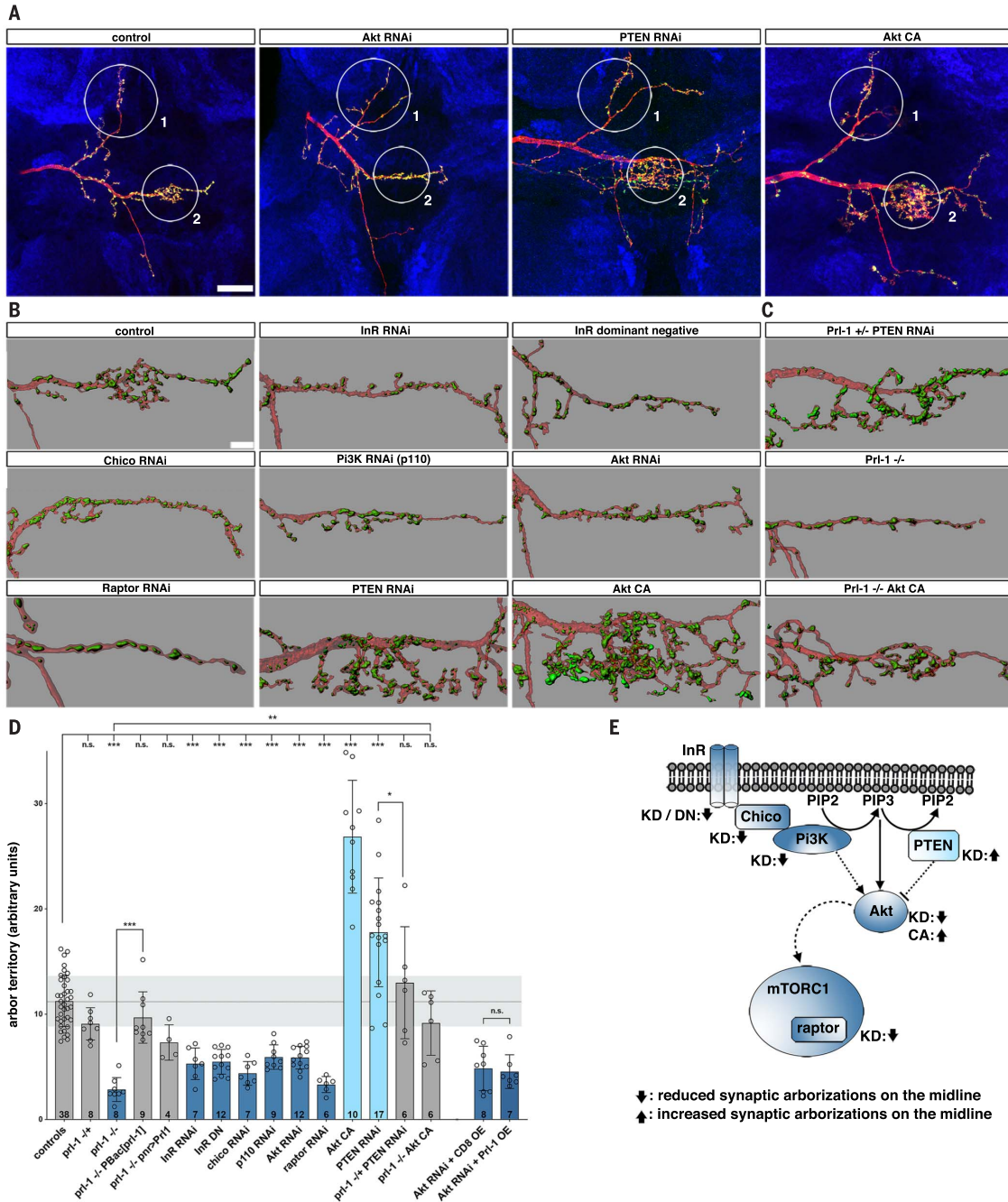
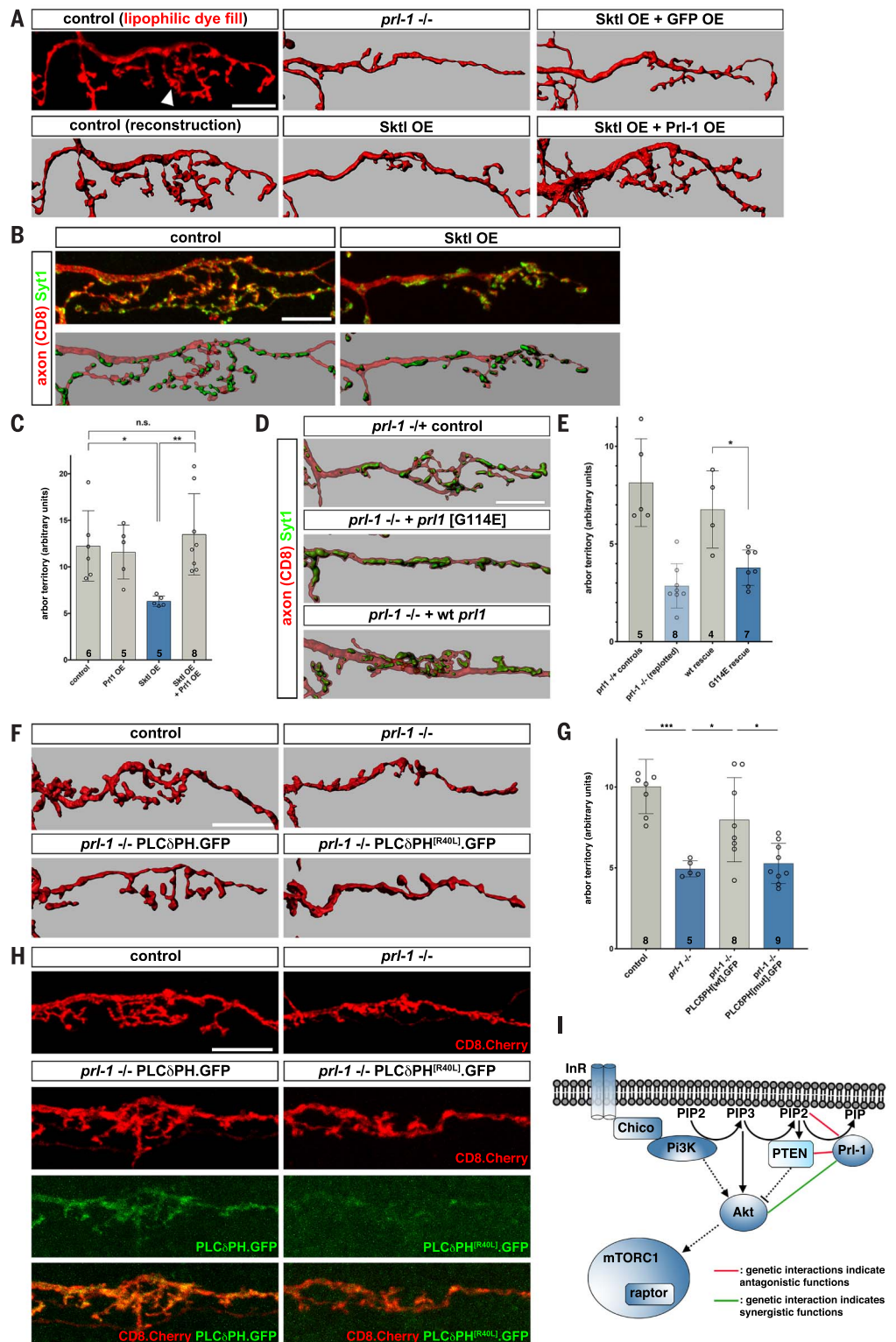


Fig. 3. The InR signaling pathway controls the formation of synapse-dense terminal arbors and interacts with *prl-1*. (A) Whole CNS projections of control DC neurons and DC neurons with reduced (Akt RNAi) or enhanced [PTEN RNAi and constitutively active (CA) Akt] Akt signaling. Note the substantial reduction (Akt RNAi) and increase (PTEN RNAi and CA Akt), respectively, in synaptic terminal arbors in the contralateral branch (target area 2), while the other axon collaterals (such as those in target area 1) are unaffected; the anterior contralateral projection, here present only in the RNAi samples, is variable also in wild-type flies. (B) Morphology of the contralateral axon branch upon the indicated manipulations in mechanosensory neurons. Visualizations of the CD8.GFP axonal marker (red) and Cherry.Syt1 presynaptic marker (green) are shown. (C) The reduction of *Prl-1* levels suppresses the PTEN phenotype (top), whereas the activation of the Akt signaling pathway rescues the *prl-1* null phenotype (bottom and middle). CA Akt was expressed only in mechanosensory neurons, which target a CNS

of reduced size (see fig. S12). (D) Quantification of terminal arbor territory in the indicated genotypes. The SD of controls is shaded in gray. Manipulations reducing the activity of the InR-Akt signaling pathway are displayed in dark blue, and manipulations enhancing the activity of the pathway are in light blue. The effects of coexpressing Akt RNAi with CD8.Cherry and *Prl-1* (the last two columns of the graph) were assessed by dye-fills and not with genetic labeling as for the rest of the genotypes. n.s., nonsignificant; * $P < 0.05$; ** $P < 0.01$; *** $P < 0.001$; ordinary one-way analysis of variance (ANOVA) with multiple comparisons. OE, overexpression. (E) Schematic of InR-Akt-mTORC1 signaling. Positive components are shaded in dark blue, and the inhibitor PTEN is in light blue. Changes in the mechanosensory neuron terminal arbor territory upon the manipulation of the gene products are indicated by arrows. KD, knockdown; DN, dominant negative; PI, phosphatidylinositol; PIP2, PI(4,5)-bisphosphate; PIP3, PI(3,4,5)-trisphosphate. Scale bars: (A), 20 μ m; (B), 5 μ m.

Fig. 4. Genetically targeting phosphoinositide levels controls terminal arbor formation.

(A) Original data and visualizations for examples of DC neuron contralateral branches in animals of the indicated genotypes. Axons were filled with a fluorescent lipophilic dye. The arrowhead points to terminal branches that are lost in *prl-1* null animals and upon the overexpression (OE) of Skt1 in mechanosensory neurons but restored upon co-overexpression of Prl-1 with Skt1. (B) The Skt1 overexpression phenotype (right) in a mechanosensory neuron labeled genetically with CD8 axonal and Syt1 presynaptic markers. Note the reduction of terminal arbor synapses. (C) Quantification of the terminal arbor territory for Skt1 and Prl-1 overexpression. n.s., nonsignificant; * $P < 0.05$; ** $P < 0.01$; Kruskal-Wallis test. (D) Visualizations for examples of mechanosensory neuron contralateral collaterals in animals of the indicated genotypes. The expression in mechanosensory neurons of a wild-type (wt) *prl-1* transgene with 5' and 3' UTRs rescues terminal arbors, whereas the expression of a UTR-containing *prl-1* transgene with the G114E mutation does not. Mechanosensory neurons project into a VNC of reduced size (fig. S16). Defects in the target area are therefore likely preventing full rescue of terminal arborizations and synapses to wild-type levels [see also (E) and (G) and Fig. 6F]. (E) Quantification of the terminal arbor territory in *prl-1* null flies rescued with different *prl-1* transgenes as in (D). See also Fig. 6 for more examples of rescue with a wild-type *prl-1* transgene. Data from *prl-1*^{-/-} flies is replotted from Fig. 3D. * $P < 0.05$, Mann-Whitney test. (F) Visualizations of dye-filled contralateral axonal projections in animals of the indicated genotypes. The expression of the PH domain of PLC δ (PLC δ PH.GFP) in mechanosensory neurons rescues terminal arborization loss in *prl-1* mutant animals (see also fig. S17 for PLC δ PH.GFP expression in mechanosensory neurons). The expression of a mutant PLC δ PH domain (PLC δ PH[R40L], where R40L is Arg⁴⁰→Lys) that does not bind to PI(4,5)P₂ does not rescue the *prl-1* phenotype. (G) Quantification of the terminal arbor territory of dye-filled contralateral collaterals in animals of the genotypes indicated in (F). * $P < 0.05$; *** $P < 0.0001$; ordinary one-way ANOVA with multiple comparisons. (H) Single-cell expression of wild-type and R40L mutant PLC δ PH.GFP, respectively, in mechanosensory neurons. CD8.Cherry is coexpressed as an axon marker, and Cherry and GFP fluorescence were



imaged. The expression of wild-type PLC δ PH.GFP cell-autonomously rescues the loss of terminal arborizations in *prl-1* null mutant animals, but the expression of PLC δ PH.GFP[R40L] does not. Wild-type PLC δ PH.GFP can be found at higher levels in the axon than the R40L mutant marker protein (see also fig. S17 for wild-type PLC δ PH.GFP localization in axons). (I) Schematic placing Prl-1 in the context of InR-Akt signaling and control of phosphatidylinositol phosphate (PIP) levels on the basis of the identified genetic interactions. All scale bars represent 10 μ m.

only mechanosensory neurons express the rescue constructs and the VNC target tissue remains mutated, with reduced neuropil size (fig. S16). In the case of the A116S mutant, we were unable to observe axonal projections of labeled mechanosensory neuron clones, suggesting a dominant effect of this mutant transgene that prevents axon growth or induces apoptosis or axon degeneration.

To further substantiate that Prl-1 leads to the dephosphorylation of PI(4,5)P2 *in vivo* and to determine whether synapse loss in mechanosensory neurons of *prl-1* null mutants is due to increased PI(4,5)P2 levels or, conversely, decreased PI(4)P levels, we used constructs expressing the pleckstrin homology (PH) domain of phospholipase C δ fused to green fluorescent protein (GFP) (PLC δ PH.GFP) (32). PLC δ PH.GFP binds to PI(4,5)P2 and prevents interactions of PI(4,5)P2 with cellular binding partners, thereby reducing functional PI(4,5)P2 levels (33). The expression of PLC δ PH.GFP, but not that of a mutant form that does not bind to PI(4,5)P2 (32), rescued the loss of terminal arborizations in *prl-1* mutants (Fig. 4, F to H). We therefore conclude that the *prl-1* null phenotype is a consequence of elevated PI(4,5)P2 in the mutant and that PLC δ PH.GFP expression can restore terminal synapse formation by blocking excessive PI(4,5)P2.

Together, our results provide evidence that Prl-1 promotes DC neuron axon arborization in a specific target area by locally influencing the phosphoinositide-dependent PI3K-PTEN signaling loop.

Prl-1 affects synapse stabilization

To gain insights into the cellular processes that cause reduced terminal synapse and arbor formation specifically in one target area of mechanosensory neurons in *prl-1* null flies, we visualized the cellular differentiation of single DC neuron compartments during development (Fig. 5). In wild-type flies, we identified three distinct stages of terminal arbor and synapse formation. In a first phase [45 to 70 hours after pupariation (apf)], the contralateral growing axon collateral extends many filopodial protrusions in all directions, including the growth direction. All these protrusions extend from the main axon shaft (Fig. 5A, top left) but are most prominently formed on the contralateral projecting axon collateral. In a second phase (60 to 75 hours apf), in which the main branch has reached the contralateral target area, filopodial protrusions are most numerous at an axon segment stretching across the midline. At this stage, new cellular processes that contain Syt1 marker protein have formed and contain additional filopodial protrusions [Fig. 5, A (middle left) and C (middle and bottom), and fig. S18A]. These satellite growth cones (34) are likely precursors of terminal synapse-bearing arborizations observed in adult animals. Lastly, in a third phase (>75 hours apf), immature filopodial protrusions and satellite growth cones disappear and are transformed into terminal synapse-bearing arbors (Fig. 5A, bottom left, and fig. S18B). In *prl-1* null flies in stage 1 and to some extent in stage 2, the develop-

ing axon collaterals and filopodial protrusions form as in wild-type controls (Fig. 5A, top right). Filopodial protrusions extend in different directions with normal abundance (Fig. 5B, left plot). Likewise, satellite growth cones with filopodia, some of which have Syt1-positive puncta, are also formed in *prl-1* mutants, and filopodia originate from these satellite growth cones (Fig. 5D and fig. S18A). However, the number of satellite growth cones per axon segment is reduced in mutant animals, and satellite growth cones extend fewer filopodial protrusions, with both characteristics leading to a net reduction in the total number of filopodial protrusions (Fig. 5B). By contrast to the reduction of filopodia originating from satellite growth cones, we did not observe a reduction of filopodia emanating from the main branch (Fig. 5B, right). These results indicate that early stages of arborization at the midline (i.e., the formation of filopodial protrusions and satellite growth cones) are not affected upon the loss of *prl-1*. By contrast, the formation or stabilization (or both) of a sufficient number of satellite growth cones is defective in *prl-1* mutants. Because Syt1 marker accumulates in satellite growth cones and filopodia extend from Syt1-positive locations, these processes may be dependent on the accumulation of synaptic material or the formation of synapses in emerging axonal processes. Lastly, in stage 3, most of the protrusions and satellite growth cones have disappeared in *prl-1* mutant axons. This suggests that in *prl-1* mutants the stabilization or consolidation of the terminal arbors as well as nascent synapses has failed and the arbors are being aberrantly retracted (Fig. 5 and fig. S18B). Thus, Prl-1 function is necessary for the stabilization or maturation of terminal synapse-bearing arbors but not the initiation or branching of axons at terminal arbors.

Compartment-specific Prl-1 enrichment

How do signaling by Prl-1 and the InR-Akt signaling activity get spatially restricted in DC axons? The branched morphologies of neurons bring many opportunities to compartmentalize subsections of the neuron. For mechanosensory neurons, additional genetic screens and characterization of other molecular pathways are required to study relevant mechanisms. However, by studying the localization of Prl-1 protein in mechanosensory neurons, we found that epitope-tagged Prl-1 expressed from a transgene is enriched in the contralateral axon collateral and is also present to a lesser degree in midline-proximal branches (Fig. 6; see also above and Fig. 1Q) and that the subcellular localization and the rescuing activity are dependent on regulatory sequences in long 5' and 3' untranslated regions (UTRs) of *prl-1* mRNAs (fig. S19). These long UTRs are essential for Prl-1 function in local synaptic arbor formation, as only HA-tagged Prl-1 proteins expressed from a transgene containing both the 5' and 3' UTRs (HA-*prl-1*.UTR^{plus}) were able to substantially rescue synaptic defects of *prl-1* mutant neurons (Fig. 6F and fig. S16). Anti-HA stainings showed that the epitope-tagged protein localized to distal axons of mechanosen-

sory neurons and was enriched in contralateral projecting branches (Fig. 6, B and D, and fig. S20). By contrast, a transgene without UTRs (HA-*prl-1*.UTR^{minus}) led to a weaker Prl-1 signal in mechanosensory neuron axons in the CNS (Fig. 6B and fig. S20). Nevertheless, without UTRs, the compartmentalized enrichment of Prl-1 is still visible in wild-type or heterozygous neurons (Fig. 6, B and C). Given that Prl proteins form homotrimers (35, 36), we reasoned that the formation of complexes between Prl-1 expressed from the endogenous locus and HA-Pr1-1 expressed from transgenes could lead to a trapping of HA-Pr1-1 protein at sites of endogenous Prl-1 enrichment (Fig. 6E, schematic). We found that the contralateral branch enrichment of protein expressed from HA-*prl-1*.UTR^{minus} was lost in a *prl-1* null mutant background and that HA-Pr1-1 localized ectopically and evenly to all axon branches of mechanosensory neurons (Fig. 6, B and C). By contrast, the localization of HA-Pr1-1 expressed from the transgene with UTRs remained compartmentalized even in the absence of endogenous protein (Fig. 6, B and D). Comparisons of protein levels in diverse wild-type and mutant backgrounds by use of fluorescence intensity is challenging. It is further complicated by the reduction of axon arbors in mutant and partially rescued samples, which thereby could indirectly contribute to a reduced fluorescence intensity. However, the ectopic redistribution of the HA-*prl-1* protein (when expressed from a transgene lacking UTRs, i.e., HA-*prl-1*.UTR^{minus}) in null mutants, which leads to an increased intensity in ipsilateral axon collaterals (unaffected in mutants), and the lack of changes in the distribution of the general membrane marker CD8. Cherry in mutants (fig. S21) provide clear evidence that Prl-1 is endogenously enriched in the contralateral projecting axon of pDC axons. Consistent with its role in the formation of terminal arbor synapses, a tagged InR protein was also localized to the contralateral projecting pDC collateral at mid-developmental stages (fig. S22).

Collectively, these results reveal a role of the *prl-1* UTRs in axon compartment-specific localization of the Prl-1 protein and show that this subcellular enrichment is likely essential for the functional specificity of Prl-1 in neurons.

Concluding remarks

In this study, we identified cell-intrinsic presynaptic mechanisms that contribute to the subcellular control of the synapse type and synapse numbers in *Drosophila* CNS axons. Compartment-specific regulation of InR signaling by Prl-1, likely by targeting of the PI3K-PTEN-dependent phosphoinositide cycle, enables the spatially restricted formation of a synapse-rich terminal arbor. This is supported by several complementary experiments. First, genetic interactions show that the loss of a single copy of *prl-1* can suppress PTEN knockdown-dependent synapse defects (Fig. 3 and fig. S11). Second, the genetic epistasis analysis, where activated Akt can rescue *prl-1* mutant defects but not vice versa, suggests that Prl-1 functions upstream of Akt (Fig. 3D and fig. S11). Third, the

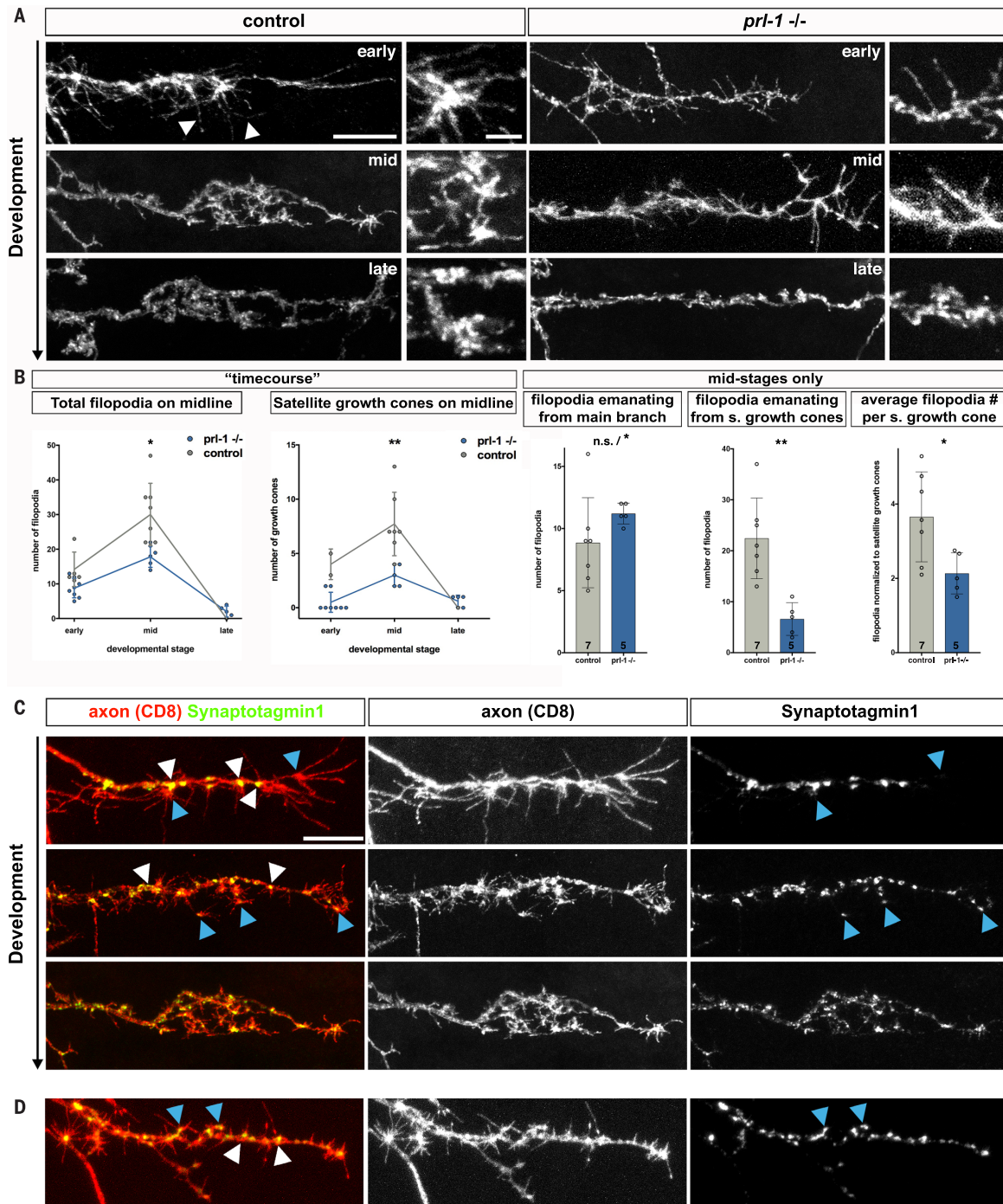


Fig. 5. Prl-1 promotes the consolidation of terminal arbors and nascent synapses. (A) Successive developmental stages of the contralateral DC neuron axon collateral in fixed control and *prl-1* null samples. In an early phase (top left) (a sample ~47 hours apf), developing branches extend long filopodial protrusions (arrowheads) and grow toward the contralateral side of the CNS. At mid-stages (middle left) (~72 hours apf), filopodium-rich satellite growth cones are visible [see (C) and also fig. S18A, arrowheads]. At late stages (bottom left) (~90 hours apf), filopodia and satellite growth cones have disappeared and terminal arbors have consolidated. In *prl-1* null animals (right panels), filopodia and satellite growth cones are initially formed but fail to accumulate and be consolidated on the contralateral branch. CNS development is delayed by ~5 to 10 hours in the mutant at these stages. Corresponding developmental stages assessed by branch growth progression, rather than by absolute timing, are displayed. Magnified

panels show examples of filopodium morphology. (B) Quantification of filopodia and satellite (s.) growth cones during different developmental stages (left panels) and at mid-stages of collateral branch formation (right panels). n.s., nonsignificant; * $P < 0.05$; ** $P < 0.01$; Mann-Whitney test. n.s./*, approximate P value of 0.06, computed exact P value of 0.048. (C) Colabeling of axon and Syt1 presynaptic marker in wild-type developing contralateral collaterals. White arrowheads indicate Syt1 accumulation on the main axon shaft, at sites where filopodia sprout. Blue arrowheads point to satellite growth cones, which are devoid of Syt1 signal at an early stage (top panels). Syt1 starts to localize to satellite growth cones at a slightly later developmental stage (middle panels). (D) *prl-1* mutant animal. Syt1 localizes to sites of filopodial sprouting (white arrowheads) and to satellite growth cones (blue arrowheads) at this early stage. Scale bars, 10 μ m (main panels) and 2.5 μ m (insets).

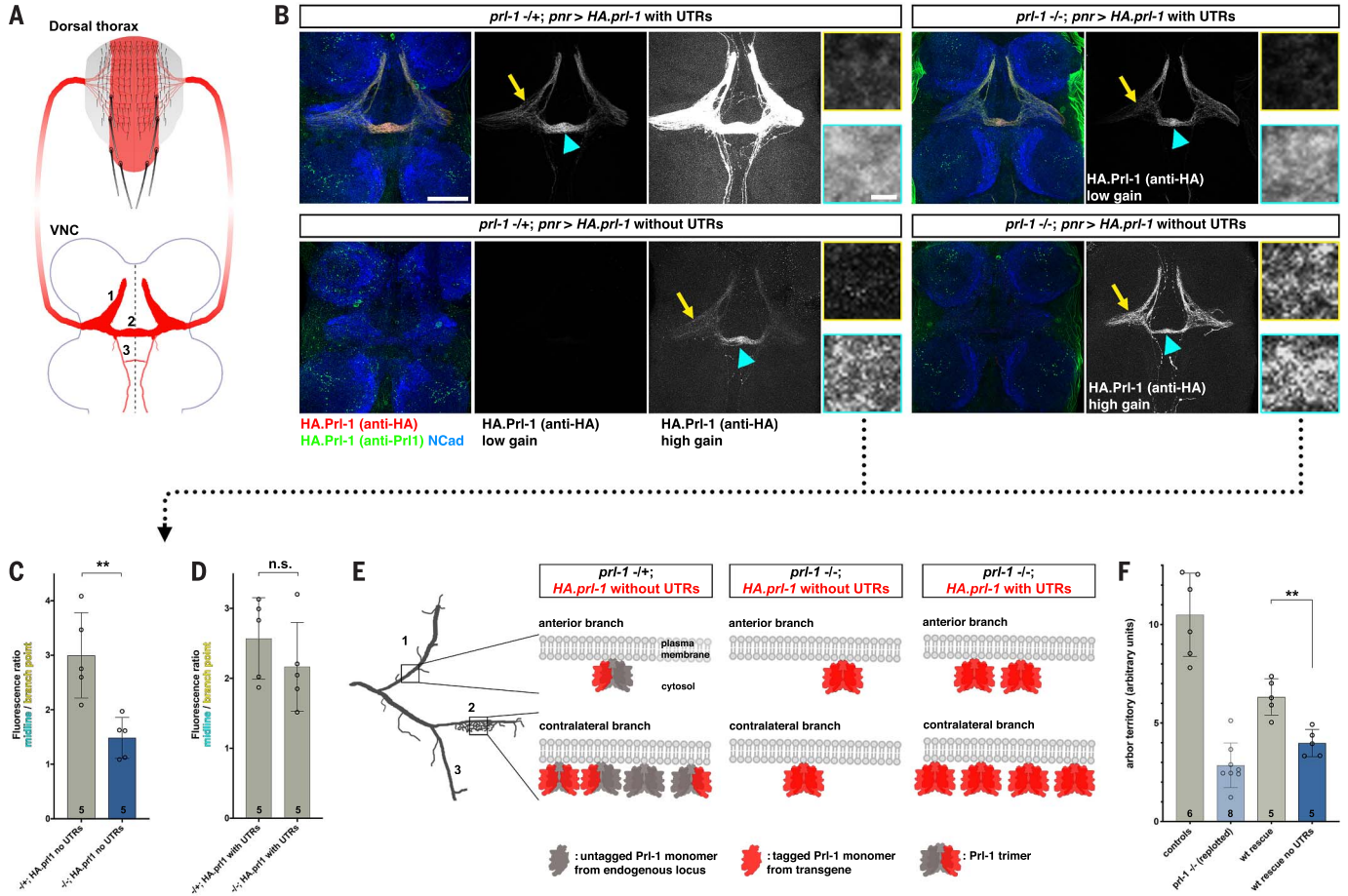


Fig. 6. *prl-1* UTRs are essential for axon localization and function.

(A) Schematic illustrating the expression pattern of *prn-gal4* (red) in adult flies. *prn-gal4*, which was used for driving UAS constructs in the experiment shown in (B), is active in the mechanosensory neurons innervating the eight large bristles (DC and SC macrochaetae) and all the small bristles (microchaetae) located in the central domain of the thorax (top, not to scale). The composite of the CNS axon projections of these neurons results in the bilateral symmetric pattern shown below; the numbering of projections corresponds to the numbering at single-axon resolution in (E) and in Fig. 1, D and L. (B) Mechanosensory neuron expression of *prl-1* transgenes with and without UTRs, detected by antibodies against Prl-1 and against the HA epitope tag, respectively. Anti-Pr1 staining is visible in CNS axon projections only when Prl-1 is expressed from a transgene with UTRs. Prl-1 protein expressed from this transgene is readily detected by staining against the HA tag in mechanosensory neuron axon projections in the CNS (top panels) (note panels showing data recorded with low and high gain, as labeled below) and is enriched in the contralateral branches (blue arrowheads) both in the presence (left panels) and in the absence (right panels) of endogenous Prl-1. By contrast, Prl-1 expressed from a transgene without UTRs (bottom panels) is expressed at much lower levels in mechanosensory neuron central axon projections (expression is visible only when imaged with high gain), and its enrichment in the contralateral branch (blue arrowheads) strongly depends on endogenously expressed Prl-1. Yellow arrows point to proximal regions of the mechanosensory neuron central projections, for direct comparison among panels. Panels on the right show high-magnification details of HA staining in the proximal regions (top) (framed in yellow) and in the contralateral branches (bottom) (framed in blue).

Signal is stronger in contralateral regions for all genotypes except for HA-Pr1 expression from a construct without UTRs in *prl-1*^{-/-} animals. Scale bars, 50 μ m (main panels) and 2 μ m (magnification panels). NCad, neural cadherin. (C) Fluorescent signal quantification of HA-Pr1 expressed from the transgene without UTRs, in a region of interest (ROI) on the contralateral branches [corresponding to magnification panels in (B)] relative to an ROI of the same size on a proximal CNS segment of the axons [magnification panels in (B)]. The enrichment on the contralateral branches is strongly reduced in animals without endogenously expressed Prl-1. ****** $P < 0.01$, Mann-Whitney test. (D) The same fluorescent signal quantification as in (C), for constructs with UTRs, reveals no significant (n.s.) (Mann-Whitney test) difference in the presence or absence of endogenously expressed Prl-1. This construct is expressed at much higher levels than the construct without UTRs [see (B)]; however, that is not reflected here, as relative values are displayed. See also fig. S21 for quantification of the membrane marker CD8:Cherry in wild-type and *prl-1*^{-/-} animals. (E) Schematic illustrating the formation of heterotrimers between Prl-1 expressed from the endogenous locus and HA-tagged Prl-1 expressed from the transgene without UTRs, leading to the enrichment of HA-Pr1 in the contralateral branch (left). In the absence of endogenous Prl-1, HA-Pr1 expressed from the transgene without UTRs is not enriched in the contralateral branch (middle). HA-Pr1 expressed from a transgene with UTRs, however, is still enriched in the contralateral branch even in the absence of endogenous Prl-1 (right), although it also accumulates in the anterior branch, possibly because of overexpression of the protein. (F) Quantification of contralateral projection arbor territory reveals that the loss of arbors cannot be rescued by a *prl-1* transgene without UTRs (see also fig. S16). ****** $P < 0.01$, Mann-Whitney test.

targeted manipulation of PI(4,5)P2 levels by overexpression of the PI(4)P 5-kinase Skittles in mechanosensory axons phenocopies the loss of Prl-1 (Fig. 4, A to C). Fourth, reducing the level of accessible PI(4,5)P2 by expressing a PI(4,5)P2-specific binding domain (PLC8PH.GFP) can suppress the Prl-1 synapse formation defects (Fig. 4, F to H). All these experiments are consistent with the model that Prl-1 targets the phosphatidylinositol 4,5-bisphosphate levels in presynaptic axon segments. However, we cannot rule out that Prl-1 only indirectly leads to the dephosphorylation of PI(4,5)P2 through an as yet unknown target in neurons. Nevertheless, this study shows that distinct lipid or phosphoinositide domains in developing axons and their likely dynamic changes contribute to the spatial specificity of CNS synapse formation.

Although the enrichment of Prl-1 protein and activity in a distinct axon branch defines this compartmentalization, it is unclear whether the localized enrichment is due to protein trafficking, protein retention, or local translation. We consider local translation a particularly attractive scenario because our data showed that the UTR sequences of *prl-1* mRNA are functionally required. Moreover, the InR pathway, which is affected by Prl-1, itself is a potent regulator of translation (37). The identification of regulatory UTR sequences in the *prl-1* mRNA that direct axon branch-specific protein localization will be a decisive tool for future studies to define the responsible cellular mechanisms.

Vertebrate phosphatases Prl-1 to -3 affect cell division or growth, as well as the metastasis of tumor cells (17, 38, 39). Analogous to the expression of *Drosophila* Prl-1, the expression of vertebrate Prl-3 in cancer cell lines is regulated at the translational level through the RNA binding protein PCBP1 and a GC-rich motif in the 5' UTR of the *prl-3* mRNA (40). However, roles for Prl proteins in CNS development have not been reported. Prl-1, Prl-2, and Prl-3 are broadly expressed in the vertebrate CNS [Allen Brain Atlas (41)]. Prl phosphatases are therefore poised to function in vertebrate brain development with effects similar to those we have shown in this study on the assembly of neuronal circuits and synapses in *Drosophila*.

REFERENCES AND NOTES

- S. Yegorov, K. Shen, Cellular and molecular mechanisms of synaptic specificity. *Annu. Rev. Cell Dev. Biol.* **30**, 417–437 (2014). doi: [10.1146/annurev-cellbio-100913-012953](https://doi.org/10.1146/annurev-cellbio-100913-012953); pmid: [25150010](https://pubmed.ncbi.nlm.nih.gov/25150010/)
- M. E. Williams, J. de Wit, A. Ghosh, Molecular mechanisms of synaptic specificity in developing neural circuits. *Neuron* **68**, 9–18 (2010). doi: [10.1016/j.neuron.2010.09.007](https://doi.org/10.1016/j.neuron.2010.09.007); pmid: [20920787](https://pubmed.ncbi.nlm.nih.gov/20920787/)
- D. A. Gibson, L. Ma, Developmental regulation of axon branching in the vertebrate nervous system. *Development* **138**, 183–195 (2011). doi: [10.1242/dev.046441](https://doi.org/10.1242/dev.046441); pmid: [21177340](https://pubmed.ncbi.nlm.nih.gov/21177340/)
- H. Schmidt, F. G. Rathjen, Signalling mechanisms regulating axonal branching in vivo. *Bioessays* **32**, 977–985 (2010). doi: [10.1002/bies.201000054](https://doi.org/10.1002/bies.201000054); pmid: [20827677](https://pubmed.ncbi.nlm.nih.gov/20827677/)
- B. Alsina, T. Vu, S. Cohen-Cory, Visualizing synapse formation in arborizing optic axons in vivo: Dynamics and modulation by BDNF. *Nat. Neurosci.* **4**, 1093–1101 (2001). doi: [10.1038/nn735](https://doi.org/10.1038/nn735); pmid: [11593233](https://pubmed.ncbi.nlm.nih.gov/11593233/)
- H. H.-W. Wong et al., RNA docking and local translation regulate site-specific axon remodeling in vivo. *Neuron* **95**, 852–868.e8 (2017). doi: [10.1016/j.neuron.2017.07.016](https://doi.org/10.1016/j.neuron.2017.07.016); pmid: [28781168](https://pubmed.ncbi.nlm.nih.gov/28781168/)
- M. P. Meyer, S. J. Smith, Evidence from in vivo imaging that synaptogenesis guides the growth and branching of axonal arbors by two distinct mechanisms. *J. Neurosci.* **26**, 3604–3614 (2006). doi: [10.1523/JNEUROSCI.0223-06.2006](https://doi.org/10.1523/JNEUROSCI.0223-06.2006); pmid: [16571769](https://pubmed.ncbi.nlm.nih.gov/16571769/)
- E. S. Ruthazer, J. Li, H. T. Cline, Stabilization of axon branch dynamics by synaptic maturation. *J. Neurosci.* **26**, 3594–3603 (2006). doi: [10.1523/JNEUROSCI.0069-06.2006](https://doi.org/10.1523/JNEUROSCI.0069-06.2006); pmid: [16571678](https://pubmed.ncbi.nlm.nih.gov/16571678/)
- J. Courchet et al., Terminal axon branching is regulated by the LKB1-NUAK1 kinase pathway via presynaptic mitochondrial capture. *Cell* **153**, 1510–1525 (2013). doi: [10.1016/j.cell.2013.05.021](https://doi.org/10.1016/j.cell.2013.05.021); pmid: [23791179](https://pubmed.ncbi.nlm.nih.gov/23791179/)
- W. D. Constance et al., Neurexin and Neuroligin-based adhesion complexes drive axonal arborisation growth independent of synaptic activity. *eLife* **7**, e31659 (2018). doi: [10.7554/eLife.31659](https://doi.org/10.7554/eLife.31659); pmid: [29504935](https://pubmed.ncbi.nlm.nih.gov/29504935/)
- B. J. Dickson, Molecular mechanisms of axon guidance. *Science* **298**, 1959–1964 (2002). doi: [10.1126/science.1072165](https://doi.org/10.1126/science.1072165); pmid: [12471249](https://pubmed.ncbi.nlm.nih.gov/12471249/)
- A. L. Kolodkin, M. Tessier-Lavigne, Mechanisms and molecules of neuronal wiring: A primer. *Cold Spring Harb. Perspect. Biol.* **3**, a001727 (2011). doi: [10.1101/cshperspect.a001727](https://doi.org/10.1101/cshperspect.a001727); pmid: [21123392](https://pubmed.ncbi.nlm.nih.gov/21123392/)
- K. Shen, C. W. Cowan, Guidance molecules in synapse formation and plasticity. *Cold Spring Harb. Perspect. Biol.* **2**, a001842 (2010). doi: [10.1101/cshperspect.a001842](https://doi.org/10.1101/cshperspect.a001842); pmid: [20452946](https://pubmed.ncbi.nlm.nih.gov/20452946/)
- O. Urwyler et al., Investigating CNS synaptogenesis at single-synapse resolution by combining reverse genetics with correlative light and electron microscopy. *Development* **142**, 394–405 (2015). doi: [10.1242/dev.115071](https://doi.org/10.1242/dev.115071); pmid: [25503410](https://pubmed.ncbi.nlm.nih.gov/25503410/)
- G. Dietzl et al., A genome-wide transgenic RNAi library for conditional gene inactivation in *Drosophila*. *Nature* **448**, 151–156 (2007). doi: [10.1038/nature05954](https://doi.org/10.1038/nature05954); pmid: [17625558](https://pubmed.ncbi.nlm.nih.gov/17625558/)
- P. Rios, X. Li, M. Köhn, Molecular mechanisms of the PRL phosphatases. *FEBS J.* **280**, 505–524 (2013). doi: [10.1111/j.1742-4658.2012.08565.x](https://doi.org/10.1111/j.1742-4658.2012.08565.x); pmid: [22413991](https://pubmed.ncbi.nlm.nih.gov/22413991/)
- S. Saha et al., A phosphatase associated with metastasis of colorectal cancer. *Science* **294**, 1343–1346 (2001). doi: [10.1126/science.1065817](https://doi.org/10.1126/science.1065817); pmid: [11598267](https://pubmed.ncbi.nlm.nih.gov/11598267/)
- D. A. Wagh et al., Bruchpilot, a protein with homology to ELKS/CAS1, is required for structural integrity and function of synaptic active zones in *Drosophila*. *Neuron* **49**, 833–844 (2006). doi: [10.1016/j.neuron.2006.02.008](https://doi.org/10.1016/j.neuron.2006.02.008); pmid: [16543132](https://pubmed.ncbi.nlm.nih.gov/16543132/)
- A. Schmid et al., Activity-dependent site-specific changes of glutamate receptor composition in vivo. *Nat. Neurosci.* **11**, 659–666 (2008). doi: [10.1038/nn.2122](https://doi.org/10.1038/nn.2122); pmid: [18469810](https://pubmed.ncbi.nlm.nih.gov/18469810/)
- J. Verdu, M. A. Buratovich, E. L. Wilder, M. J. Birnbaum, Cell-autonomous regulation of cell and organ growth in *Drosophila* by Akt/PKB. *Nat. Cell Biol.* **1**, 500–506 (1999). doi: [10.1038/70293](https://doi.org/10.1038/70293); pmid: [10587646](https://pubmed.ncbi.nlm.nih.gov/10587646/)
- A. A. Friedman et al., Proteomic and functional genomic landscape of receptor tyrosine kinase and Ras to extracellular signal-regulated kinase signaling. *Sci. Signal.* **4**, rs10 (2011). doi: [10.1126/scisignal.2002029](https://doi.org/10.1126/scisignal.2002029); pmid: [22028469](https://pubmed.ncbi.nlm.nih.gov/22028469/)
- H. Wang et al., PRL-3 down-regulates PTEN expression and signals through PI3K to promote epithelial-mesenchymal transition. *Cancer Res.* **67**, 2922–2926 (2007). doi: [10.1158/0008-5472.CAN-06-3598](https://doi.org/10.1158/0008-5472.CAN-06-3598); pmid: [17409395](https://pubmed.ncbi.nlm.nih.gov/17409395/)
- Y. Jiang et al., Phosphatase PRL-3 is a direct regulatory target of TGFβ in colon cancer metastasis. *Cancer Res.* **71**, 234–244 (2011). doi: [10.1158/0008-5472.CAN-10-1487](https://doi.org/10.1158/0008-5472.CAN-10-1487); pmid: [21084277](https://pubmed.ncbi.nlm.nih.gov/21084277/)
- V. McParland et al., The metastasis-promoting phosphatase PRL-3 shows activity toward phosphoinositides. *Biochemistry* **50**, 7579–7590 (2011). doi: [10.1021/bi201095z](https://doi.org/10.1021/bi201095z); pmid: [21806020](https://pubmed.ncbi.nlm.nih.gov/21806020/)
- B. Vanhaesebroeck, L. Stephens, P. Hawkins, PI3K signalling: The path to discovery and understanding. *Nat. Rev. Mol. Cell Biol.* **13**, 195–203 (2012). doi: [10.1038/nrm3290](https://doi.org/10.1038/nrm3290); pmid: [22358332](https://pubmed.ncbi.nlm.nih.gov/22358332/)
- A. Klippel, W. M. Kavanaugh, D. Pot, L. T. Williams, A specific product of phosphatidylinositol 3-kinase directly activates the protein kinase Akt through its pleckstrin homology domain. *Mol. Cell Biol.* **17**, 338–344 (1997). doi: [10.1128/MCB.17.1.338](https://doi.org/10.1128/MCB.17.1.338); pmid: [8972214](https://pubmed.ncbi.nlm.nih.gov/8972214/)
- R. B. Campbell, F. Liu, A. H. Ross, Allosteric activation of PTEN phosphatase by phosphatidylinositol 4,5-bisphosphate. *J. Biol. Chem.* **278**, 33617–33620 (2003). doi: [10.1074/jbc.C300296200](https://doi.org/10.1074/jbc.C300296200); pmid: [12857747](https://pubmed.ncbi.nlm.nih.gov/12857747/)
- S. Knirr, A. Santel, R. Renkawitz-Pohl, Expression of the PI4P 5-kinase *Drosophila* homologue *skittles* in the germline suggests a role in spermatogenesis and oogenesis. *Dev. Genes Evol.* **207**, 127–130 (1997). doi: [10.1007/s004270050099](https://doi.org/10.1007/s004270050099); pmid: [27747405](https://pubmed.ncbi.nlm.nih.gov/27747405/)
- B. A. Hassan et al., *skittles*, a *Drosophila* phosphatidylinositol 4-phosphate 5-kinase, is required for cell viability, germline development and bristle morphology, but not for neurotransmitter release. *Genetics* **150**, 1527–1537 (1998). pmid: [9832529](https://pubmed.ncbi.nlm.nih.gov/9832529/)
- S. Claret, J. Jouette, B. Benoit, K. Legent, A. Guichet, PI(4,5)P2 produced by the PI4P5K SKTL controls apical size by tethering PAR-3 in *Drosophila* epithelial cells. *Curr. Biol.* **24**, 1071–1079 (2014). doi: [10.1016/j.cub.2014.03.056](https://doi.org/10.1016/j.cub.2014.03.056); pmid: [24768049](https://pubmed.ncbi.nlm.nih.gov/24768049/)
- M. P. Myers et al., The lipid phosphatase activity of PTEN is critical for its tumor suppressor function. *Proc. Natl. Acad. Sci. U.S.A.* **95**, 13513–13518 (1998). doi: [10.1073/pnas.95.23.13513](https://doi.org/10.1073/pnas.95.23.13513); pmid: [9811831](https://pubmed.ncbi.nlm.nih.gov/9811831/)
- P. Verstreken et al., Tweek, an evolutionarily conserved protein, is required for synaptic vesicle recycling. *Neuron* **63**, 203–215 (2009). doi: [10.1016/j.neuron.2009.06.017](https://doi.org/10.1016/j.neuron.2009.06.017); pmid: [19640479](https://pubmed.ncbi.nlm.nih.gov/19640479/)
- D. Raucher et al., Phosphatidylinositol 4,5-bisphosphate functions as a second messenger that regulates cytoskeleton-plasma membrane adhesion. *Cell* **100**, 221–228 (2000). doi: [10.1016/S0092-8674\(00\)81560-3](https://doi.org/10.1016/S0092-8674(00)81560-3); pmid: [10660045](https://pubmed.ncbi.nlm.nih.gov/10660045/)
- D. Descenzo et al., Slit and receptor tyrosine phosphatase 69D confer spatial specificity to axon branching via Dscam1. *Cell* **162**, 1140–1154 (2015). doi: [10.1016/j.cell.2015.08.003](https://doi.org/10.1016/j.cell.2015.08.003); pmid: [26317474](https://pubmed.ncbi.nlm.nih.gov/26317474/)
- J.-P. Sun et al., Structure and biochemical properties of PRL-1, a phosphatase implicated in cell growth, differentiation, and tumor invasion. *Biochemistry* **44**, 12009–12021 (2005). doi: [10.1021/bi050919i](https://doi.org/10.1021/bi050919i); pmid: [16142898](https://pubmed.ncbi.nlm.nih.gov/16142898/)
- J.-P. Sun et al., Phosphatase activity, trimerization, and the C-terminal polybasic region are all required for PRL1-mediated cell growth and migration. *J. Biol. Chem.* **282**, 29043–29051 (2007). doi: [10.1074/jbc.M703537200](https://doi.org/10.1074/jbc.M703537200); pmid: [17656357](https://pubmed.ncbi.nlm.nih.gov/17656357/)
- X. M. Ma, J. Blenis, Molecular mechanisms of mTOR-mediated translational control. *Nat. Rev. Mol. Cell Biol.* **10**, 307–318 (2009). doi: [10.1038/nrm2672](https://doi.org/10.1038/nrm2672); pmid: [19339977](https://pubmed.ncbi.nlm.nih.gov/19339977/)
- Q. Zeng et al., PRL-3 and PRL-1 promote cell migration, invasion, and metastasis. *Cancer Res.* **63**, 2716–2722 (2003). pmid: [12782572](https://pubmed.ncbi.nlm.nih.gov/12782572/)
- A. Q. O. Al-Aidaros, Q. Zeng, PRL-3 phosphatase and cancer metastasis. *J. Cell. Biochem.* **111**, 1087–1098 (2010). doi: [10.1002/jcb.22913](https://doi.org/10.1002/jcb.22913); pmid: [21053359](https://pubmed.ncbi.nlm.nih.gov/21053359/)
- H. Wang et al., PCBP1 suppresses the translation of metastasis-associated PRL-3 phosphatase. *Cancer Cell* **18**, 52–62 (2010). doi: [10.1016/j.ccr.2010.04.028](https://doi.org/10.1016/j.ccr.2010.04.028); pmid: [20609352](https://pubmed.ncbi.nlm.nih.gov/20609352/)
- E. S. Lein et al., Genome-wide atlas of gene expression in the adult mouse brain. *Nature* **445**, 168–176 (2007). doi: [10.1038/nature05453](https://doi.org/10.1038/nature05453); pmid: [17151600](https://pubmed.ncbi.nlm.nih.gov/17151600/)
- W. Fouquet et al., Maturation of active zone assembly by *Drosophila* Bruchpilot. *J. Cell Biol.* **186**, 129–145 (2009). doi: [10.1083/jcb.200812150](https://doi.org/10.1083/jcb.200812150); pmid: [19596851](https://pubmed.ncbi.nlm.nih.gov/19596851/)

ACKNOWLEDGMENTS

We thank L. Saucedo (University of Pudget Sound) for UAS-*prl-1* flies; H. Stocker (ETH Zurich) for UAS-*InR.CFP* flies; P. Verstreken (VIB KU Leuven) for UAS-PLC8PH.GFP flies; K. Vints and A. Kremer (VIB Biologem Core) for electron microscopy; M. Dirix, B. Yan, J. Yan, and Z. Huang (VIB KU Leuven) for help with experiments; and P. Vanderhaeghen (VIB KU Leuven), B. Hassan (ICM Paris), J. de Wit (VIB KU Leuven), and M. Holt (VIB KU Leuven) for critically reading the manuscript. Fly stocks obtained from the Bloomington *Drosophila* Stock Center (NIH P400018537) and from the Vienna *Drosophila* Resource Center (VDRRC) were used in this study. Some monoclonal antibodies were obtained from the Developmental Studies Hybridoma Bank (created by the NICHD of the NIH and maintained at The University of Iowa). **Funding:** This work was supported by VIB funds (D.S.) and project grants from Belgian FWO and EOS (30913351, SYNET) programs (D.S.) and from the Swiss National Science Foundation to O.U. (PBEP3_130209 and PZ00P3_161448). **Author contributions:** O.U. and D.S. designed experiments; O.U., A.I., S.V., S.S., and A.M. performed experiments; O.U. and D.S. analyzed and interpreted the data, wrote the manuscript, and acquired funding; and all authors read and commented on the manuscript. **Competing interests:** The authors declare no competing interests. **Data and materials availability:** All data are available in the main text or the supplementary materials.

SUPPLEMENTARY MATERIALS

science.sciencemag.org/content/364/6439/eaau9952/suppl/DC1
Materials and Methods
Figs. S1 to S22
Table S1
References (43–63)
Movie S1

3 August 2018; accepted 29 March 2019
[10.1126/science.aau9952](https://doi.org/10.1126/science.aau9952)

Branch-restricted localization of phosphatase Prl-1 specifies axonal synaptogenesis domains

Olivier Urwyler, Azadeh Izadifar, Sofie Vandenberghe, Sonja Sachse, Anke Misbaer and Dietmar Schmucker

Science **364** (6439), eaau9952.
DOI: 10.1126/science.aau9952

Compartmentalization of axons

Neurons can spread branches far and wide across the central nervous system. One neuron can simultaneously contact several other neurons, amplifying network complexity. Studying the *Drosophila* brain, Urwyler *et al.* found that not all axon branches are the same, even within one neuron (see the Perspective by Falkner and Scheiffele). A membrane-anchored phosphatase functions within a subset of axon branches to regulate synapse formation. Thus, the pattern of synapses on one neuron is not random but rather is spatially restricted according to subcompartments in the axon.

Science, this issue p. eaau9952; see also p. 437

ARTICLE TOOLS

<http://science.sciencemag.org/content/364/6439/eaau9952>

SUPPLEMENTARY MATERIALS

<http://science.sciencemag.org/content/suppl/2019/05/01/364.6439.eaau9952.DC1>

RELATED CONTENT

<http://science.sciencemag.org/content/sci/364/6439/437.full>

REFERENCES

This article cites 63 articles, 26 of which you can access for free
<http://science.sciencemag.org/content/364/6439/eaau9952#BIBL>

PERMISSIONS

<http://www.sciencemag.org/help/reprints-and-permissions>

Use of this article is subject to the [Terms of Service](#)